A Min-time Analysis of Three Trajectories with Curvature and Nonholonomic Constraints Using a Parallel Parking Criterion

Douglas Lyon
Chair, Computer Engineering Department
Fairfield University
Fairfield, CT 06430
Lyon@docjava.com, http://www.docjava.com

Abstract

This paper presents a comparison of three s-shaped curves for parallel parking a car subject to nonholonomic constraints. The comparison is based on the rate at which the car approaches the curb (the parking criterion). The curves (two circular arcs, a cosine curve and a quintic) are shown to accommodate an initial and final position, but only the quintic accommodates initial and final curvature. The time penalty in straightening out the wheels at the maneuver end-points (or midpoint) causes the other curves to be suboptimal.

Representative examples of the curves are shown. Also illustrated is the effect of the turning radius of the car on the time required to park it.

1. Problem Statement and Motivation

Given a nonholonomically constrained car in or near a parking space, we need to find a trajectory that minimizes the time to park. The problem of parking a car is a special case docking problem. The docking problem is constrained in this manner to focus attention on curves that allow movement to a specific goal and to focus on techniques for comparison between curves and their parking times.

There are several reasons to solve this type of problem. The first is the product potential for car manufacturers, consistent with the advent of common sensor and microprocessor technologies. A second is the contribution to the area of reference-path generation with nonholonomically constrained tracking. Prototype cars have been developed that make use of cosine curves in their parking trajectory [Paromtchik]. This study shows that the cosine curve is suboptimal with respect to the quintic.

The rest of the paper is structured as follows; Section 2 describes the derivation of a quintic as the quintessential parking curve. Section 2.1 uses a geometric and algebraic approach to formulate the polynomial. Section 2.2 shows how nonholonomic constraints map the curvature of a reference path (i.e., the quintic) into a front-wheel angle for the car as a function of path-length. Section 2.3 shows an example path and how lateral excursion into the space is a quadratic function of maneuver room. Section 3 compares the quintic with two other s-shaped curves using the rate of traversal into the space as a function of time (the parking criterion). Section 4 describes the contribution of this study to other work in the field. Finally, section 5 summarizes the results and gives some guidance for future work.

2. Derivation of the Quintic

The car follows a path that is subject to nonholonomic constraints. The deflection of the front of the car during a maneuver (called the *Max Y-Deflection*) is a function of the available maneuver room.

Let:

$k5 \equiv$ curvature of the quintic,

$L \equiv$ length of the car,

$PSL \equiv$ Parking Space Length,

$PSW \equiv$ Parking Space Width,

$(x_f, y_f) \equiv$ position of the front of the car and

$(x_r, y_r) \equiv$ position of the rear of the car.

The parameters and variables are shown in Figure 2-1. Our simplified model assumes that the bumper-to-bumper length and the length of the car are the same lengths. We can reduce the *PSL* in order to take the difference into account, should this be needed.

The car's centerline excursion at the maneuver end-points is called the Y-Deflection and this is also a function of maneuver room. Figure 2-1 shows the car and parking space geometry.

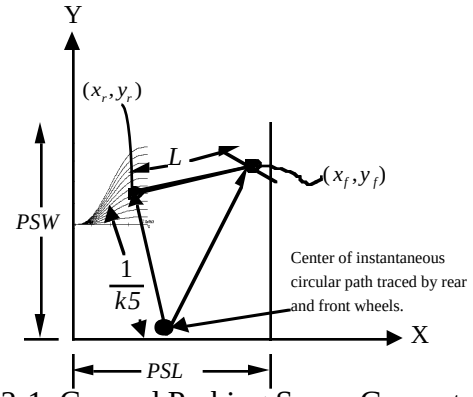

Figure 2-1. Car and Parking Space Geometry
Sample maneuvers are shown.
Scale: 1 cm = 2 meters, in the x-direction, 1 cm = 0.5 meters in the y-direction.

The car must avoid collision with the walls of the parking space (i.e., the car in front and the car in back) and fit into the parking space. The rear-path curvature must be strictly less than the maximum-allowable curvature ($|k5| < k_{max}$)[1]. The rear path has specified slope and curvature at the maneuver end-points.

2.1 Derivation by Docking Constraints

This section presents a derivation of a quintic for the rear trajectory. We will show that a quintic is the minimum order polynomial able to give sufficient degrees of freedom and comply with the docking constraints.

The rear path during a single maneuver is represented as a (single-valued) function $y_r = f(x_r)$. The general form of a quintic is given by

$$y_r(x_r) = a_5 x_{re}^{\ 5} + a_4 x_{re}^{\ 4} + a_3 x_{re}^{\ 3} + a_2 x_{re}^{\ 2} + a_1 x_{re} + a_0 \qquad (2.1)$$

where:

---

[1] Here 'strictly' is used to mean that the constraint applies to all points on the curve.

$x_{re} \equiv x_r / x_e$

$(x_r, y_r) \equiv$ position of the rear of the car,

$(x_r, y_r) = (\mathrm{x_e}, y_e)$, when maneuver is complete,

$(x_r, y_r) = (0, a_0)$, at the maneuver start and

$x_r \in [0\mathsf{K}\ x_e]$, so that $x_{re} \in [0\mathsf{K}\ 1]$.

$\theta 5 \equiv$ car orientation when the rear of the car follows a quintic,

$\phi 5 \equiv$ the steering - wheel angle when the rear of the car follows a quintic,

$k5 \equiv$ curvature of the quintic,

$s5 \equiv$ length of the path traveled by the front wheel when the rear of the car follows a quintic,

$ds5 \equiv$ small change in $s5$,

$d\mathrm{s_r} \equiv$ small path length change for the rear wheel,

$(x_r, y_r) \equiv$ position of the rear of the car,

$(x_f, y_f) \equiv$ position of the front of the car,

$r \equiv$ turning radius of the front wheel of the car and

$L =$ distance between front and back wheels.

$(x_{rL=llfgkjdslfk}, y_r) = (\mathrm{x_e}, y_e)$, when maneuver is complete and

$(x_r, y_r) = (0, a_0)$, at the maneuver start, so that $x_{re} \in [0\mathsf{K}\ 1]$.

$x_{re} \equiv x_r / x_e$

and is subject to constraints on slope

$$y_r^{'} = \frac{dy_r}{dx_r}, y_r^{'}(0) = y_r^{'}(x_e) = 0 \tag{2.2}$$

and curvature

$$k5(0) = k5(x_e) \tag{2.3},$$

where

$$k5(x_r) = \frac{y_r^{''}}{\left[1 + \left(y_r^{'}\right)^2\right]^{3/2}} \tag{2.4}$$

so that

$$y_r^{''}(0) = y_r^{''}(x_e) = 0 \tag{2.5}$$

is necessary and sufficient for (2.3) to be true.

Applying (2.2) and (2.5) to (2.1) yields

$$y_r(x_r) = y_e\left(6x_{re}{}^5 - 15x_{re}{}^4 + 10x_{re}{}^3\right) \tag{2.6}$$

Substituting (2.6) into (2.4) results in

$$k5(x_r) = y_e\left(120\frac{x_r^3}{x_e^5} - 180\frac{x_r^2}{x_e^4} + 60\frac{x_r}{x_e^3}\right)\left[1 + y_e^2\left(30\frac{x_r^4}{x_e^5} - 60\frac{x_r^3}{x_e^4} + 30\frac{x_r^2}{x_e^3}\right)^2\right]^{-\frac{3}{2}} \tag{2.7}$$

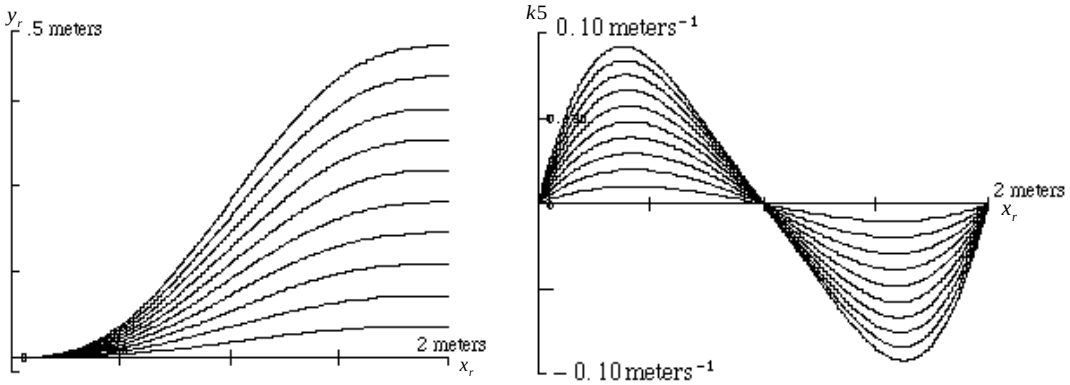

Figure 2.1-1. Family of Quintics and Respective Curvatures. The curves have varying amplitude with zero slope and curvature at the maneuver end-points.

Figure 2.1-1 shows a family of quintics and their corresponding curvatures.

The location and value of the curvature maximum varies as a function of the amplitude. In Figure 2.1-1, x_e = 2 meters. Note that x_r varies from 0 to x_e and that the only degree of freedom left is y_e. This corresponds to the Y-deflection of the quintic at the maneuver end-points and is limited by the maximum permissible curvature for the rear of the car (a function of the limited turning radius). Each quintic has a zero derivative and curvature at the end-points as well as different amplitudes and curvature maximums. There is only one quintic with a curvature maximum, over the feasible range of x_r, equal to $k_{\max}$. The maximum curvature, $k_{\max}$, and the maneuver room, x_e, are car and parking-space specific. There is no analytic closed-form solution for the maximum of (2.7) as far as we know. Even when the maneuver room is known in advance, solving for the zeros of the derivative of (2.7) requires finding the roots of quintics.

The next section shows how to use the nonholonomic constraints to guide the steering of the front of the car in order for the rear of the car to trace out the quintic path.

2.2 Derivation by Nonholonomic Constraints

Consider Figure 2.2-1, where

$\theta 5 \equiv$ car orientation when the rear of the car follows a quintic,

$\phi 5 \equiv$ the steering - wheel angle when the rear of the car follows a quintic,

$k5 \equiv$ curvature of the quintic,

$s5 \equiv$ length of the path traveled by the front wheel when the rear of the car follows a quintic,

$ds5 \equiv$ small change in $s5$,

$ds_r \equiv$ small change in the length of the path traveled by the rear wheel when the rear of the car follows a quintic,

$(x_r, y_r) \equiv$ position of the rear of the car,

$(x_f, y_f) \equiv$ position of the front of the car,

$r \equiv$ turning radius of the front wheel of the car and

$L =$ length of the car.

The car has pose $(x_f, y_f, \theta 5)$ and steering-wheel angle $(\phi 5)$. Explicit functional notation is omitted for brevity. This notation is based on the work of Barraquand and Latombe [Latombe et al. 1989].

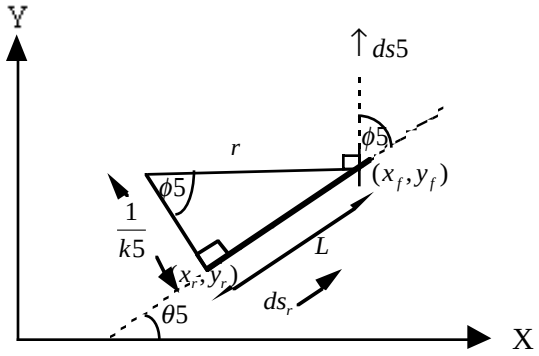

Figure 2.2-1. 2-D Car States
The turning radius of the car is measured by the perpendicular distance between a ray emanating from the rear axle of the car and front wheel.

Car orientation, $\theta 5$, and steering-wheel angle, $\phi 5$, are in radians. The front of the car (x_f, y_f) and length, L, are measured in meters.

The angle, $\theta 5$, the car makes with the X-axis is called the car orientation. The angle of the front wheel with respect to the main axis of the car, $\phi 5$, is called the steering-wheel angle. The distance traversed by the front wheel is denoted $s5$. The kinematic equations of car motion are

$$\frac{d\theta 5}{ds5} = \frac{1}{r} = \frac{\sin \phi 5}{L} \tag{2.8}$$

and

$$\frac{dy_f}{dx_f} = \tan(\theta 5 + \phi 5) \tag{2.9}.$$

Equations (2.8) and (2.9) arise because the point at which the wheels touch the ground has zero velocity with respect to the car (the no-slip condition). The no-slip condition requires car travel in the direction of its wheels. The steering-wheel angle, $\phi 5$, is measured relative to the car orientation. The velocity of the front of the car is tangent to the front wheel. The proof is in [Lyon 1991].

The rear wheel is always tangent to the main axis of the car and this results in

$$\frac{dy_r}{dx_r} = \tan(\theta 5) \tag{2.10}.$$

The rear of the car is fixed relative to the front of the car and this results in

$$\begin{aligned} x_r &= x_f - L\cos\theta 5 \\ y_r &= y_f - L\sin\theta 5 \end{aligned} \tag{2.11}.$$

For the rear path to track a curve whose curvature is $k5$, subject to constraints (2.8) and (2.9), we must set the steering-wheel angle so that

$$\phi 5 = \arctan(k5\ L) \tag{2.12}.$$

Given constant steering angle, the front and rear of the car trace the arc of a circle, and orientation changes as a linear function of $s5$ [Barraquand et al. 1989]. Thus, the curvature of the path for the rear of the car maps directly to the front-wheel angle. By extension, (2.12) can be used to guide the car along any path, once the path curvature is known and assuming that the physical limits (i.e., turning radius of the car) are not exceeded.

2.3 Examples

In this section we solve the initial boundary value problem subject to equations (2.8-2.12). Test vehicle measurements showed that the maximum of $\phi = 0.526$ radians. Using $L = 2.7$ meters a maximum value of 0.223 meters^{-1} for the curvature of the rear of the car results; this correlates with the measured 0.26 meters^{-1} from field tests. Assuming a car X-deflection of 2.4 meters, the quintic Y-deflection, with a curvature maximum of 0.223 meters^{-1}, is 0.23 meters. This is found by using the bisection method of Bolzano [Matthews].

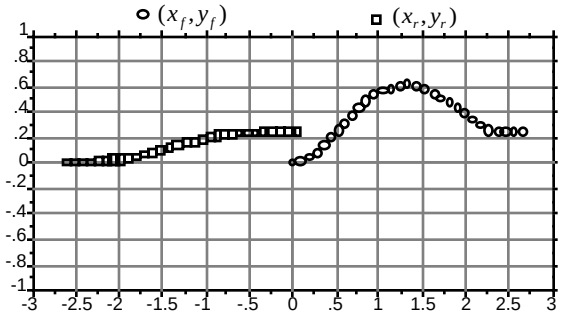

Figure 2.3-1. Example Maneuver
All units are in meters. We show the solution to the nonholonomically constrained initial-value problem.

Figure 2.3-1 shows the numerical solution and the tracks of the center of the front and rear of the car as a function of the path length of the front of the car.

Figure 2.3-2 shows that the car orientation and curvature are zero at the maneuver end-points, and this means that the car is parallel to the curb and that the front wheel is straight.

Tabulated results show that the maximum curvature is 0.223 meters^{-1}, the Y-component of the final rear deflection is 0.23 meters and that the maximum steering-wheel angle is 0.526 radians. Thus, the state variables that describe the car motion are feasible.

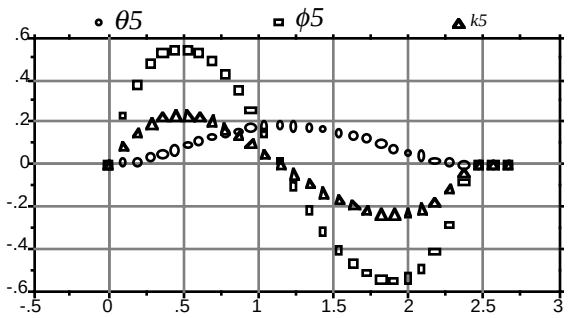

Figure 2.3-2. Example Angles and Curvature.
The steering-wheel angle, car orientation and curvature are zero at the maneuver end-points. The curvature for the rear of the car, as described by the quintic, (k5) is in meters^{-1}. The steering-wheel angle and car orientation are in radians.

Several simulations were used to measure the maximum Y-deflection for various values of maneuver room. The maximum Y-deflection is the peak lateral excursion required for a maneuver. A graphical summary and quadratic approximation to the data is shown in Figure 2.3-3.

If the car approaches the curb, the parking space width cannot be considered infinite and the car must back into the space. If the car were to pull forward, without sufficient space between the car and the curb, the car would mount the curb.

Simulation predicts the Y-deflection at the maneuver end-points for various values of maneuver room (i.e., *PSL-L*). A graphical summary and a quadratic approximation to the data is shown in Figure 2.3-3. The deflection into the parking space is a quadratic function of the available maneuver room. Simple circular arcs also yield a quadratic deflection as a function of *PSL-L*.

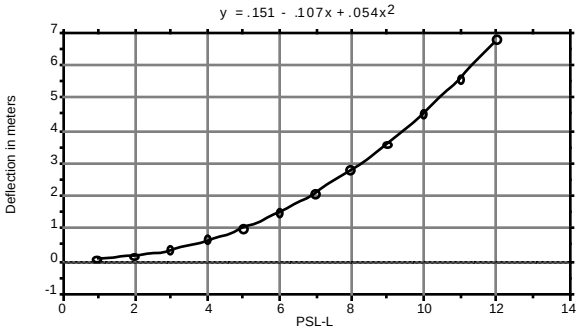

Figure 2.3-3. Y-Deflection vs. PSL-L.
Several experiment show that the deflection of the car at the maneuver end-points is almost quadratic in PSL-L.

3. Comparison with other curves

This section compares 3 parking curves (two circular arcs, a cosine curve, and a quintic) to determine their suitability for parking. We consider:

1. two linked circular arcs,
2. the cosine curve and
3. the quintic.

The curves are C^0 continuous. The cosine curve and the quintic are C^n continuous. Two linked circular arcs are piece wise C^n continuous with a single discontinuity. These are also the continuity classes of the respective curvatures.

We assume that the car is at rest at the maneuver end-points. All trajectories described use a single acceleration and deceleration, except for steering at rest.

3.1 Steering At Rest With Two Accelerations

Steering at rest requires turning the front wheel as far as possible toward the curb, moving the car to the midpoint of the path, stopping the car; and then turning the front wheel all the way in the other direction, in preparation for the second half of the maneuver. The absolute value of the curvature is constant throughout the maneuver. The car starts and finishes at rest and parallel to the curb. A curvature singularity occurs at the maneuver midpoint. At this point the car must come to rest with the front wheels turned all the way in the other direction. This rest at the maneuver midpoint requires that the car decelerate and accelerate an extra time.

The car follows a path whose trace is produced by the following equation:

$$y = \begin{cases} \sqrt{r^2 - x^2}, & 0 \le x \le \dfrac{PSL - L}{2} \\ -\sqrt{r^2 - \left[x - (PSL - L)\right]^2} + \sqrt{4r^2 - (PSL - L)^2}, & \dfrac{PSL - L}{2} < x \le PSL - L \end{cases}$$

Where

$$x \in [0, PSL - L].$$

See [Lyon 1991] for a proof.

3.2. Steering At Rest With One Acceleration

The trace of steering at rest with two accelerations is identical to that of steering at rest with one acceleration. The difference is that steering at rest with one acceleration does not incur a time penalty by stopping in the middle of the maneuver and turning the steering wheel.

Steering at rest, with one acceleration, is a kind of maneuver that employs bang-bang curvature control with a zero switching time. This maneuver is optimal in the sense that it minimizes the time to park. This establishes a theoretical temporal parking bound that can never be attained in real-life parking situations.

3.3 The Cosine Curve

The cosine curve is a continuous-steering solution. Like steering at rest, the cosine curve has non-zero curvature at the maneuver end-points. This is important because the time it takes to turn the wheels is nontrivial. The formula to generate the cosine curve is

$$y = a\cos(\pi u)$$

where

$$u = x / (PSL - L),$$

$$x \in [0, PSL - L]$$

and

$$a = -k_{\max}(PSL - L)^2 / \pi^2.$$

The cosine curvature maximum appears at integral multiples of π/2 radians, and has a symbolic solution for the amplitude in terms of the curvature maximum

The length of the cosine curve is

$$L_{\cos}(PSL - L) = \int_0^{PSL-L} \left(1 + \left(\frac{d}{dx}\left(a\cos(\pi u)\right)\right)^2\right)^{1/2} dx.$$

This formula requires numerical solution. The rate at which the car will park is

$$R_{\cos}(PSL - L, r, a_{\max}) = \frac{y_{\cos}(PSL - L, r)}{t_{\cos}(PSL - L, a_{\max})}.$$

Where

$$y_{\cos}(PSL - L, r) = (PSL - L)^2 / (\pi r)$$

is the amount of deflection obtained from the cosine curve during a parking maneuver and

$$t_{\cos}(PSL - L, r, a_{\max}) = 2\left(\frac{L_{\cos}(PSL - L, r)}{a_{\max}}\right)^{-1/2}$$

is the time needed to perform the maneuver.

3.4. The Quintic

In this section, we constrain the quintic so that the curvature and orientation are zero at the maneuver end-points.

Curvature specification at the curve end-points will save front-wheel alignment time and reduce tire wear. Assuming end-point curvature is zero, then

$$k(0) = k(PSL - L) = 0 .$$

The quintic is designed using knowledge about constraints and is a minimum-order polynomial with end-point curvature and slope control. Assuming the general form of a quintic, each constraint is enforced until the following formula results:

$$y = au^5 + (5/2)au^4 - (5/3)au^3 - y0$$

where

$$u = x / (PSL - L),$$
$$x \in [0, PSL - L]$$

and *a* is a numerically computed function of k_{max}.

3.5. Results

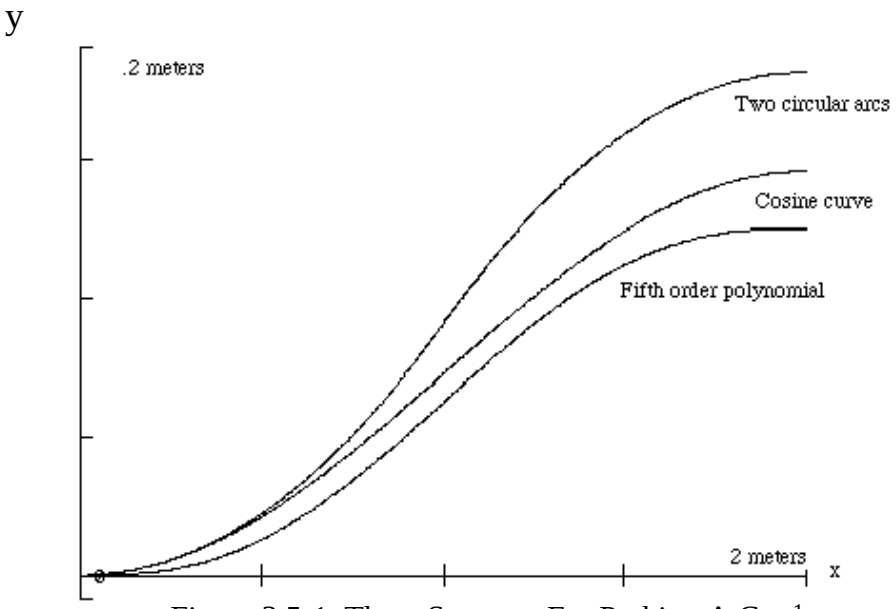

Figure 3.5-1. Three S-curves For Parking A Car.[1]
The maximum curvature for each curve is 0.2 meters -1.

We compare the paths with respect to the time it takes the car to park. Figure 3.5-1 shows three curvature constrained S-curves. The curves shown have a maximum curvature of 0.2 meters $^{-1}$. Finite curvature constraints limit the deflection per maneuver (called Δy_{max}). Comparison based on Δy_{max} indicates steering at rest dominates other curves, due to its minimized curvature. We make the assumption that the time it takes to turn the front wheel is zero, and compute the time necessary to traverse each curve subject to maximum acceleration and deceleration constraints.

[1] Distortion in printing causes elongation of curves.

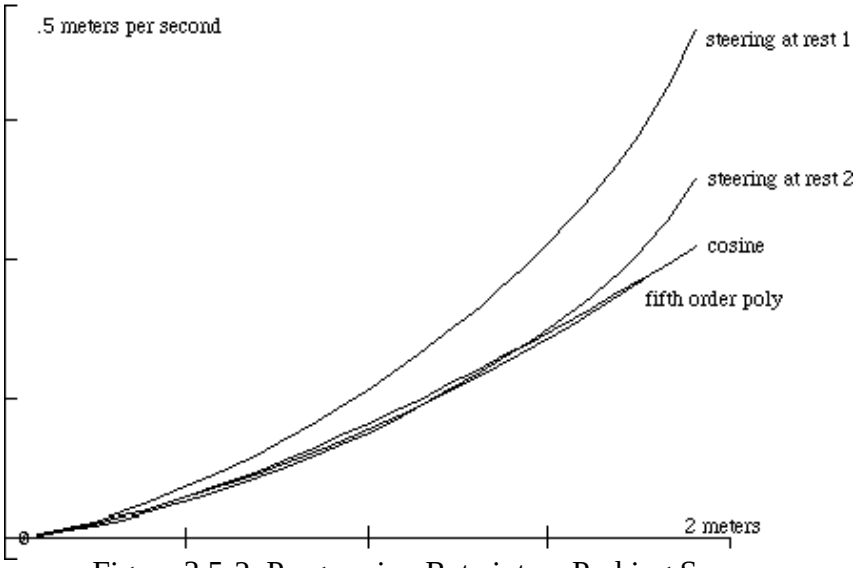

Figure 3.5-2. Progression Rate into a Parking Space.
Within a certain range the quintics performance dominates the other curves. Steering at rest with one acceleration is impossible, the car stops to steer at rest.

Figure 3.5-2 shows the lateral velocity $(\Delta y_{\max} / t_{path})$ vs. *PSL* for each path, and this indicates time-optimal progress into the space. Figure 3.5-2 shows that the rate at which a car progresses is a function of the available maneuvering space. The maximum acceleration is $a_{\max} = 1.5 \text{ m} / \text{s}^2$. Other curves dominate the quintic when neglecting front-wheel reorientation at the maneuver end-points.

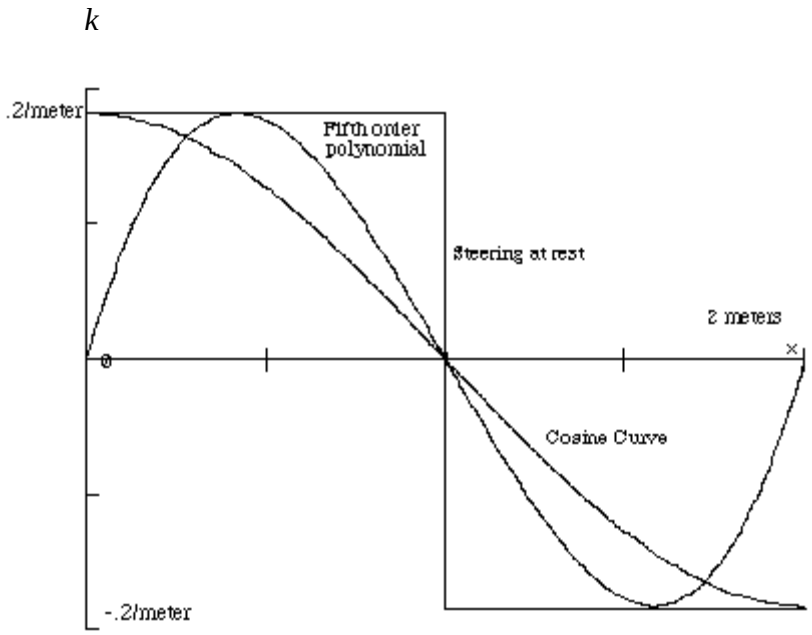

Figure 3.5-3. S-Curve Curvatures.
The Cosine Curve and Steering at Rest incur a penalty at the maneuver end-points that the quintic eliminates.

Figure 3.5-3 shows the quintic has a curvature equal to zero at the maneuver end-points. In the quintic, the time needed to turn the front-wheel at the beginning and end of the maneuver is eliminated. Steering at rest and the cosine curve lump extreme front wheel motion at the maneuver end-points. Steering at rest also has extreme wheel motion at the center-point of the maneuver. In contrast, the quintic starts and ends with the wheels parallel to the curb.

We now repeat the comparison using median values for the car turning radius, length, and parking space length. The median values are r=3.1 meters, L=4.9 meters and PSL=5.2 meters, according to [Lyon 1991]. The maneuvering space is PSL-L=0.3 meters! It is not reasonable to assume that the parking space will be exactly the mid-point between the small car space and the big car space. To be more realistic, we study PSL in the range from 5.2 meters to 11 meters. At 9.1 meters the numeric computations for the quintic become ill-conditioned. Figure 3.5-4 shows the track diagram of the front and rear of a car that follows the quintic curve.

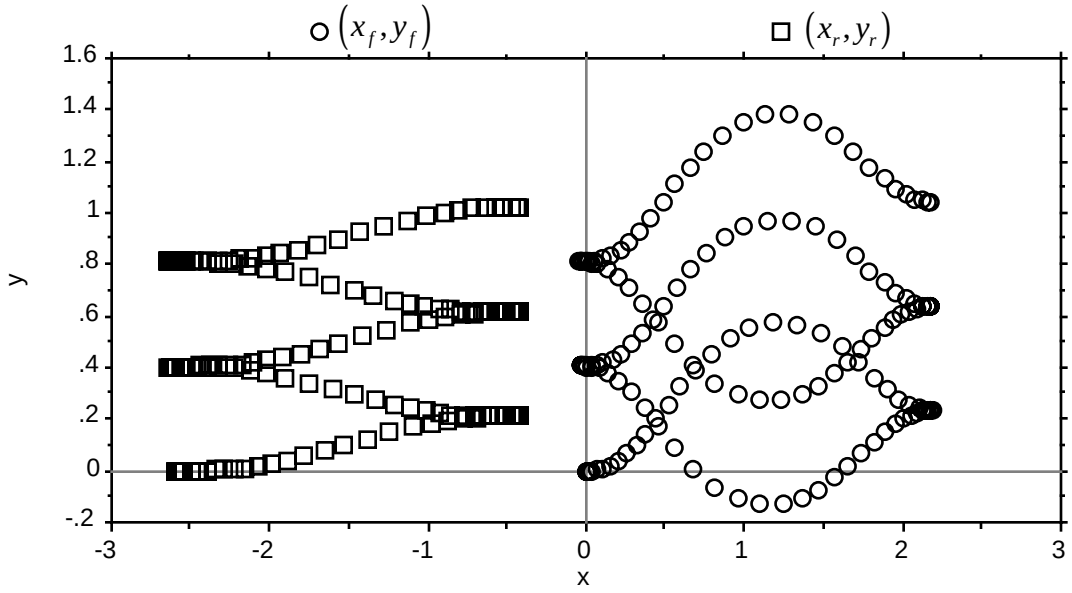

Figure 3.5-4. Curvature Tracking.
All units are in meters.

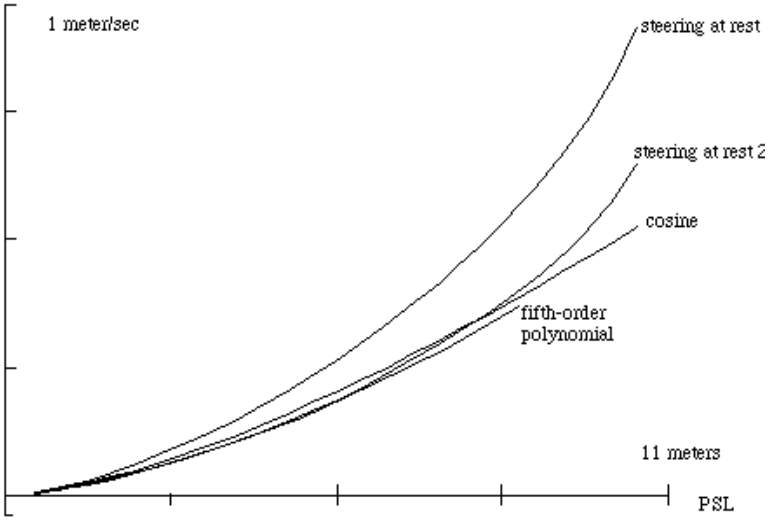

Figure 3.5-5 Rate at which Car Approaches the Curb
The dominating curves appear to have only marginal advantages over each other.

In figure 3.5-5, the parking space length (*PSL*) is treated as a parameters that enables the selection of the fastest means of parking the car. The speed of the parking process is based on the rate of parking space penetration (i.e., the lateral speed of the car as it works it way into the space). That is, it is the distance traveled toward the curb after a maneuver, divided by the time it takes to perform the maneuver. Figure 3.5-5 shows that, when neglecting front-wheel reorientation at the maneuver end-points, other curves continue to dominate the quintic. However, even with very fast steering it takes at least two to four seconds to turn the steering wheel from one extreme to another. This makes the quintic a time optimal trajectory for parking. If on the other hand, we sought to minimize the number of maneuvers, rather than parking time, steering at rest dominates the other curves.

4. Other work in the field

The idea for using a reference path for the car to track is not new and there are other curves that are, in some sense, better. For example, the cubic spiral is a smoother path than the quintic [Kanayama et Al. 1988]. The drawback of this curve is that it has non-zero curvature at the maneuver end-points. The advantage is that the curve minimizes the jerk exerted on passengers.

The idea of using a quintic for car-like maneuvers is not new [Nelson 1989]. However, the formulation described here differs from Nelson's in that it is constrained by the maximum deflection permissible, given the curvature constraints. In addition a comparison is made between the quintic and other parking curves.

The idea of parallel parking a car with nonholonomic constraints is not new, either [Paromtchik]. However, Paromtchik, and Laugier did not try to compare their trajectories with others. We have shown that the cosine curve is, in general, slower to park than the quintic and requires excessive steering.

In the past, we have seen complicated approaches such as the nonholonomically constrained configuration-space search [Barraquand et al. 1989], neural nets [Widrow et al. 1990] or fuzzy control [Sugeno et al. 1985] for parallel parking a car.

The draw-back of configuration-space search is that it requires considerable computational resource. We have introduced a new, simple parking criterion, so that the selection of a path becomes computationally tractable. Other techniques (i.e., fuzzy and neural network control) run the risk of being suboptimal with respect to the parking criterion. With these approaches, the operator's skill becomes the limiting factor. In addition, the use of the parking criterion has led to fore-knowledge of the time it will take to park. This information is not available with the fuzzy or neural network control approaches. Literature shows that the neural-network approach requires thousands of training sessions [Widrow et al. 1990].

Figure 2.3-3 shows when to substitute a smaller *PSL-L* to match the maximum Y-deflection to the available lateral maneuver room. Aside from intercept control [Burke 1975], there is no known method to bring a robot *as close as possible* to an obstacle.

5. Summary

The parking problem motivates the investigation into specialized curve constraints and a novel comparison technique. In the average case of parking, a continuous steering strategy (quintic) dominates a lumped steering strategy (steering at rest and the cosine curve).

Deflection into the parking space in a single maneuver and the rate of parking-space penetration are approximated by quadratic functions of the available maneuver room. This result follows from the constant acceleration and deceleration used to maneuver the car.

In this paper we have used slope and curvature constraints to derive a quintic, and this was shown to provide a faster means of parking than other curves. We also derived the relationship between the steering-wheel angle and the rear-path curvature using nonholonomic constraints.

Curvature was shown to be minimal for the linked arcs, evenly distributed for the cosine curve and lumped toward the end-points for the quintic that allows curve end-point specification of curvature and slope.

The solution to the parking problem led to the development of a criterion for the suitability of curves for parking. This criterion is based on the rate at which a car penetrates into the space and it is the *parking criterion*.

The quintic is a minimum-order polynomial designed to comply with the docking constraints. The quintic saves time by leaving the car and steering wheel parallel with the curb at the maneuver end-points. There are no other curves known have steering-wheel control at maneuver end-points.

The nonholonomic constraints allow the computation of the steering-wheel angle as a function of the rear-path curvature. A car will have a rear path that is, in general, different from but isomorphic with the front path.

Safe paths in the presence of obstacles can be generated by joining the spines of a Voronoi diagram [Preparata et Al. 1985] with quintics to create composite paths. These paths would be centered between obstacles as well as have curvature and slope continuity and this has interesting applications for space and underwater docking. Using the hexidecitree data structure [Lyon 1986] rather than the Voronoi diagram could also lead to a solution to the multiagent path planning problem and this has applications in aircraft control and animation language.

6. Literature Cited

[Barraquand et Al. 1989] Barraquand, J. and Latombe, J. *Robot Motion Planning: A Distributed Representation Approach*, STAN-CS-89-1257, Department of Computer Science, Stanford University Stanford, CA, 94305, (1989)

[Burke 1975] Burke, J., October 20, 1975. *Understanding Intercept Control*, Mitre Technical Report MTR-3133, The Mitre Corporation, Bedford, MA.

[Kanayama et Al. 1988] Kanayama, Y. and Hartman, B. *Smooth Local Path Planning for Autonomous Vehicles*, TRCS88-15, Department of Computer Science, University of California, Santa Barbara, CA. (1988)

[Latombe et al. 1989] Latombe, J. and Barraquand, J.. "On Nonholonomic Mobile Robots and Optimal Maneuvering", *Proceedings of the IEEE International Symposium on Intelligent Control*, IEEE, NY, NY. (1989)

[Lyon 1986] Lyon, D. "An N-Space Subdivision Algorithm for Generating Trajectories", *Robot and Expert Systems Conference*, Instrument Society of America, Research Triangle Park, NC. (1986)

[Lyon 1990] Lyon, D. "Ad hoc and Derived Curves for Parallel Parking a Car", *Symposium on Advances in Intelligent Systems*, Proceedings Volume 1388-04, SPIE, Bellingham, WA. (1990)

[Lyon 1991] Lyon, D. *Parallel Parking with Nonholonomic Constraints*, Ph.D. Thesis, Computer and Systems Engineering, Rensselaer Polytechnic Institute, Troy, NY, 12181, (1991)

[Lyon 2002] Lyon, D., "Sensor Fusion and Bang-Bang Control with Nonholonomic Constraints", JSME International Journal, Series C, Vol. 45, No. 2, (2002).

[Matthews 1987] Matthews, J., 1987. *Numerical Methods*, Prentice-Hall, Inc., Englewood Cliffs, NJ.

[Nelson et al. 1988] Nelson, W. and Cox, I. "Local Path Control for an Autonomous Vehicle", *IEEE International Conference on Robotics and Automation*, IEEE, NY, NY, pp. 1504–1510, (1988)

[Nelson 1989] Nelson, W., "Continuous-Curvature Paths for Autonomous Vehicles", *IEEE International Conference on Robotics and Automation*, IEEE, NY, NY, pp. 1260–1264, (May 14, 1989).

[Paromtchik] I. E. Paromtchik, and C. Laugier, "Motion Generation and Control for Parking an Autonomous Vehicle, " Proc. of the IEEE Int. Conf. on Robotics and Automation, Minneapolis, USA, (April 22-28, 1996), pp. 3117-3122. http://citeseer.nj.nec.com/paromtchik96motion.html

[Preparata et Al. 1985] Preparata, F. and Shamos, M., *Computational Geometry, An Introduction*, Springer-Verlag, NY, NY, (1985)

[Sugeno et al. 1985] Sugeno, M. and Murakami, K. “An Experimental Study On Fuzzy Parking Control Using a Model Car”, *Industrial Applications of Fuzzy Control*, North Holland Publishing, NY, NY (1985)

[Widrow et al. 1990] Widrow, B. and Nguyen, D. “Improving the learning speed of 2-layer neural networks by choosing initial values of the adaptive weights”, *Int. Joint Conf. on Neural Networks*, pp. 21–26, (July 17, 1990).

[Whitehead 1990] Whitehead, J., March, 1990. “Rear Wheel Steering Dynamics Compared to Front Steering”, *Journal of Dynamic Systems, Measurement, and Control* , Volume 112, pp. 88–93.